

Article

Untargeted Metabolomic Profiling of *Fructus Chebulae* and *Fructus Terminaliae Billericae*

Yuman Song  and Hede Gong * 

College of Geography and Ecotourism, Southwest Forestry University, Kunming 650224, China; songyuman2003@outlook.com

* Correspondence: gonghede@swfu.edu.cn

Abstract: This study aims to identify the differences in metabolites between *Fructus Chebulae* (FC) and *Fructus Terminaliae Billericae* (FTB). Untargeted metabolomics was used to analyze differentially expressed metabolites (DEMs) with ultra-performance liquid chromatography–electrospray ionization–tandem mass spectrometry (UPLC-ESI-MS/MS). A grand total of 558 metabolites were detected, with 155 in positive ion mode and 403 in negative ion mode. Further differential analysis yielded 110 and 87 significantly different metabolites, which were mainly polyphenols, flavonoids, terpenoids, and alkaloids. Analysis of KEGG data showed that differentially expressed metabolites (DEMs) in both positive and negative ion modes were found to be enriched in 5 and 18 metabolic pathways, respectively, with metabolic pathways being the most enriched among them. In sum, this study reveals the differential metabolic profiles of FC and FTB and provides support for their further applications in traditional Chinese medicine.

Keywords: *Fructus Chebulae*; *Fructus Terminaliae Billericae*; metabolomics; differential metabolites; KEGG analysis



Citation: Song, Y.; Gong, H. Untargeted Metabolomic Profiling of *Fructus Chebulae* and *Fructus Terminaliae Billericae*. *Appl. Sci.* **2024**, *14*, 3123. <https://doi.org/10.3390/app14073123>

Academic Editors: Claudio Medana and Aljaz Medic

Received: 7 March 2024

Revised: 3 April 2024

Accepted: 3 April 2024

Published: 8 April 2024



Copyright: © 2024 by the authors. Licensee MDPI, Basel, Switzerland. This article is an open access article distributed under the terms and conditions of the Creative Commons Attribution (CC BY) license (<https://creativecommons.org/licenses/by/4.0/>).

1. Introduction

Fructus Chebulae (FC), commonly known as chebulic myrobalan, is the dried mature fruit of *Terminalia chebula* Retz, a plant of the Combretaceae family [1]. Feverfew is frequently encountered in Yunnan, Guangdong, and Guangxi and is widely utilized in traditional Chinese medicine (TCM), Tibetan medicine, Ayurveda, and various other traditional healing practices. Known as the king of medicine, traditional plant medicine is widely utilized across the globe [2]. It is not only used for medicinal purposes but it also serves as a healthy food for throat clearing. It is an important raw material in the tanning industry [3]. The FTB is a variant of the FC, mainly distributed in western Yunnan, Myanmar (Pegu, wool cotton to Dian Na Saleng), and other places.

The 2015 edition of the *Pharmacopoeia of the People's Republic of China*, Volume I, covers various uses of raw and processed FC in traditional Chinese medicine. As stated in *Encountering the Sources of the Classic of Materia Medica*, “FC is bitter and astringent and decreases converged qi; raw FC clears the lung and stops coughing, while roasted FC protects the intestines and prevents diarrhea”. Traditional medicine and modern pharmacological studies have indicated that FC contains numerous active ingredients including tannic acids, phenolic acids, triterpenes, polysaccharides, and volatile oils. These compounds have been shown to exert diverse pharmacological effects, such as antibacterial, vasoconstrictive, immune-enhancing, antitumor, and free radical-scavenging activities [4,5].

The desiccated fruits of *Terminalia chebula* can be classified as FC and *Fructus Terminaliae Billericae* (FTB), with distinctions in physical characteristics, effectiveness, and medicinal attributes. The physical characteristics of the young seeds (varieties) and the original varieties include thick copper and flat hairs on young branches and leaves, longer bracts than flowers, a barren calyx, and a glabrous ovary when young. The fruit is ovate and less than

2.5 cm long [6]. At present, there are few studies on small hair seeds at home and abroad, and only a few documents focus on the dry mature fruit [7]. FC and FTB contain tannin, phenolic acids, triterpenoids, and flavonoids as their primary chemical constituents, all of which possess pharmacological properties like antioxidant, liver protection, antibacterial, and antitumor effects [8]. The extract and active ingredients mainly protect the liver, kidney, and heart by scavenging free radicals, thereby affecting oxidase activity, antioxidative stress response, and other mechanisms, and play an antioxidant role [9,10]. It exerts an antibacterial effect by inhibiting bacterial cell protease activity, inhibiting cell membrane efflux function, and inhibiting nucleic acid synthesis [11,12]. It exerts its antitumor effect by affecting the passage of tumor cell apoptosis signal transduction, protein synthesis and function of tumor cells, nucleic acid biosynthesis of tumor cells, and synergistic efficacy with antitumor drugs [13,14]. At present, the research work on FC mainly focuses on the active ingredients, pharmacological effects, clinical application, and processing of such plants. Few studies have been conducted on FC and FTB; in particular, the analysis of the chemical composition between the two has not been reported. The two differences in the efficacy of the ko and micro may be different. The current research aimed to analyze the variations in the metabolites between FC and FTB through untargeted metabolomics using UPLC-ESI-MS/MS, with the goal of laying a foundation for future studies on FC in traditional Chinese medicine and the chemical industry.

2. Materials and Methods

2.1. Materials and Reagents

FTB and FC were identified according to their leaf shapes and fruit morphologies (October 2022, Yongde County, Lincang, China). Methanol (CNW Technologies, Düsseldorf, Germany, LC-MS grade), acetonitrile (CNW Technologies, Germany, LC-MS grade), formic acid (SIGMA, Livonia, MI, USA, LC-MS grade), and FMOC-L-2-Chlorophe (Shanghai, China, Hengbai Biotech Co., Ltd., $\geq 98\%$ purity) were utilized.

2.2. Instruments and Equipment

The study utilized the Vanquish ultra-high performance liquid chromatography system (Thermo Fisher Scientific, Waltham, MA, USA), Orbitrap Exploris 120 high-resolution mass spectrometer (Thermo Fisher Scientific, MA, USA), Heraeus Fresco17 low-temperature centrifuge (Thermo Fisher Scientific, MA, USA), BSA124S-CW analytical balance (Sartorius, Shanghai, China), JXFSTPRP-24 grinder (Shanghai, China, Jingxin Industrial Development Co., Ltd.), Ming Che D24 UV water purifier (Merck Millipore, Darmstadt, Germany), YM-080S sonicator (Shenzhen, China, Fangao Microelectronics Co., Ltd.), and ACQUITY UPLC BEH C18 chromatography column (Waters, MA, USA).

2.3. Experimental Methods

2.3.1. Extraction of Metabolites

The samples were freeze-dried in a lyophilizer and then pulverized into powder using a grinder operating at 60 Hz for 30 s. The sample powder was weighed at a quantity of 100 mg and then combined with 500 μL of extraction solution (methanol–water ratio of 4 to 1, with an internal standard concentration of 10 $\mu\text{g}/\text{mL}$). After vortexing for 30 s, the mixture was homogenized at 45 Hz for 4 min, followed by sonication for 1 h in an ice-water bath. It was then incubated at $-40\text{ }^\circ\text{C}$ for 1 h before being centrifuged at $4\text{ }^\circ\text{C}$ for 15 min at 12,000 rpm (equivalent to a centrifugal force of $13,800\times g$). After passing through a microporous membrane with a pore size of 0.22 μm , the supernatant was combined with 20 μL of each sample to create the quality control sample. All samples were stored at $-80\text{ }^\circ\text{C}$ for subsequent testing.

2.3.2. Sample Analysis

UPLC-ESI-MS/MS was performed using the following settings. The UPLC BEH C18 chromatography column (1.7 $\mu\text{m} \times 2.1 \times 100\text{ mm}$) was used with an injection volume

of 5 μ L. The mobile phases consisted of 0.1% formic acid aqueous solution (A) and 0.1% formic acid aqueous solution (B). The sheath gas flow rate was set to 30 Arb, while the auxiliary gas flow rate was 10 Arb. The ion transfer tube and evaporator temperatures were both maintained at 350 °C. The resolution was 60,000 for full MS and 15,000 for MS/MS; collision energy was set at 16/38/42 in NCE mode; spray voltage was set at 5.5 kV (positive) or -4 kV (negative).

2.3.3. Statistical Analysis

All experiments were repeated at least three times, and the results were expressed as mean standard deviation (SD). The data were analyzed using Origin 2021, Excel2020, and IBM SPSS Statistics V. 25. 0. The significance of the difference was analyzed by the Duncan test, and the significance level was <0.05 . The KEGG metabolic pathway was analyzed using the Sichuan biological cloud platform (<https://www.omicstudio.cn/doc/1152> accessed on 20 January 2023) for correlation analysis, principal component analysis (PCA), and to draw heat maps.

2.4. Data Processing

XCMS was used to import the unprocessed data from mass spectrometry for correcting retention times and identifying, extracting, integrating, and aligning peaks. Peaks containing MS/MS data were identified using a custom-built MS/MS database (custom-built database of Shanghai, China Biotree Biomedical Technology Co., Ltd.) and the corresponding fragmentation pattern-matching algorithm.

3. Results

3.1. Phenotypic Characterization

FC and FTB grow in the same environment and during the same season (Figure 1) but have significantly different morphologies. FC leaves are narrower with darker colors and distinct veins, and the fruits are green with dark spots and are uniform in size. In contrast, FTB leaves are wider with lighter color, brown spots, and distinct veins, and the fruits have a lighter hue with distinct brown patches and come in various sizes. The morphological characteristics of leaves and fruits that differ between FC and FTB are shown in Figure 1. Table 1 displays variations in the weights of leaves and fruits between FC and FTB (See Supplementary Information Table S1 for details).

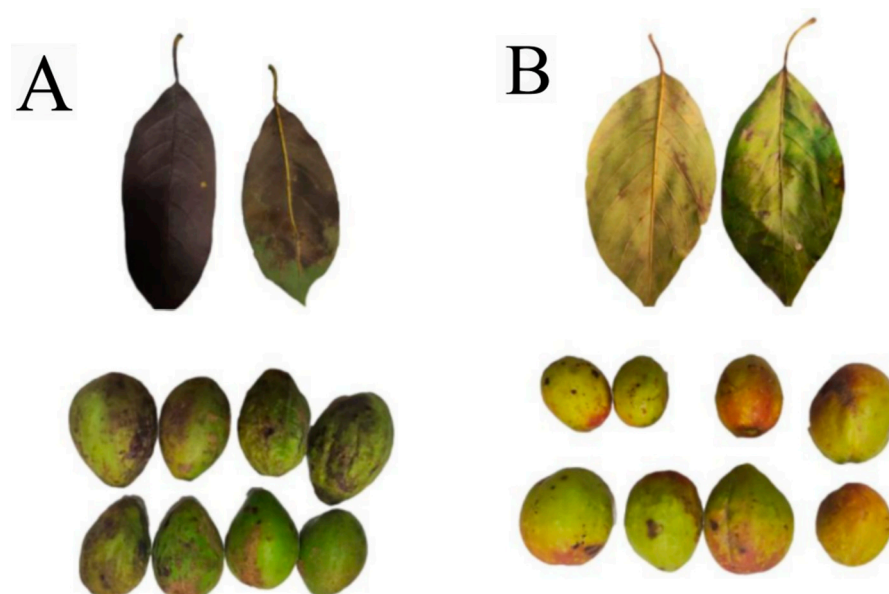


Figure 1. Morphological characteristics of leaves and fruits of FC (A) and FTB (B).

Table 1. Leaf and fruit mass of FTB and FC.

Species Name	Fresh Leaf Mass (g)	Dry Leaf Mass (g)	Fresh Fruit Mass (g)	Dry Fruit Mass (g)
FTB	1.27 ± 0.11 ^b	0.78 ± 0.01 ^b	13.25 ± 5.06 ^a	5.17 ± 1.65 ^a
FC	1.69 ± 0.07 ^a	0.85 ± 0.02 ^a	10.20 ± 1.58 ^a	3.91 ± 0.58 ^a

Different lowercase superscript letters in the same column indicate significant differences ($p < 0.05$).

3.2. Metabolite Detection

Untargeted metabolomics analysis was conducted on FC and FTB to further explore their differences. The horizontal coordinate represents the retention time. The ordinate represents the response signal value (peak area); the positive and negative ions were tested for 30 min. In total, 571 signal values were measured in positive ion mode, and 220 signal values were measured in negative ion mode (See Supplementary Tables S2 and S3 for details). FC and FTB produced highly similar metabolite peak patterns as visualized on total ion chromatograms (TICs) but with significantly different peak values (Figure 2). FC reached a peak value of 3×10^3 in positive ion mode and $>3 \times 10^3$ and $<3.5 \times 10^3$ in negative ion mode, whereas FTB had a peak value of 4×10^3 in positive ion mode and 2.4×10^3 in negative ion mode. The peak intensity of various peaks fluctuated relative to each other. For example, the peak at about 7 min in positive ion mode was significantly higher in FC than FTB, and the peak at 17.6 min was significantly lower in FC than FTB. This indicates a notable disparity in metabolite levels between FC and FTB.

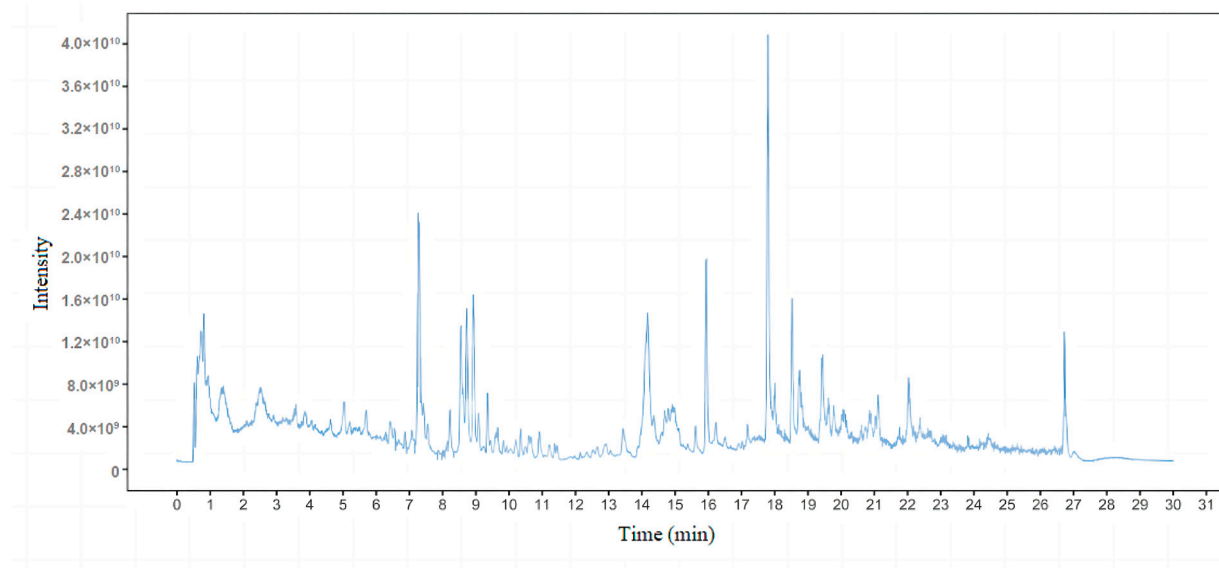
Metabolite Identification and PCA Analysis

The identities of metabolites in the samples were determined by matching the characteristics of the metabolites, such as molecular mass (± 10 ppm), secondary fragmentation spectra, and retention time, to those in the custom-built MS/MS database. A grand total of 558 metabolites were detected, with 155 in the positive ion mode and 403 in the negative ion mode. The classifications of the metabolites are visualized in pie charts in Figure 3. The filters according to vip value and p -value are as follows: 6-Aminocaproic acid; L-Alanine; DL-Alanine; L-Arginine; L-Phenylalanine; D-(+)-Phenylalanine; DL-Phenylalanine; Phenethyl alcohol; 2-Phenylethanol; Quassin. Testosterone is a major contributor to PC. Various metabolite classes are depicted by the colors in the pie charts, while the sizes of the sections indicate the relative amounts of metabolites. The majority of identified metabolites were terpenoids, flavonoids, phenols, phenylpropionic acids, or alkaloids. Terpenoids are an essential class of compounds in medicinal herbs with expectorant, antitussive, wind-dispelling, analgesic, and various other physiological activities. Natural terpenoids have been shown to exert antitumor activities by regulating host biological functions [15]. Flavonoids are widely spread substances that have a wide range of biological properties, including protection for the heart, antibacterial and antiviral effects, anticancer properties, antioxidant capabilities, anti-inflammatory properties, pain relief, and liver protection [16]. Phenolic compounds, which are secondary metabolites, can be found in various parts of plants such as fruits, skins, roots, and leaves, with their makeup differing between plant species. One of the most important physiological activities of phenolic compounds is the inhibition of free radicals and delay of damage [17]. Phenylpropionic acids, an important class of phenylpropanoids, are naturally occurring organic acids containing C6-C3 units, including cinnamic acids and phenyllactic acids. Many phenylpropionic acids have antioxidant, bacteriostatic, immune-enhancing, antitumor, antiviral, anti-inflammatory, and lipid-lowering activities as well as therapeutic effects in cardiovascular diseases [18]. There are many compounds with medicinal values among alkaloids. For example, matrine has cardiogenic and anti-arrhythmic functions, and aconitine can dilate the coronary artery and blood vessels in the extremities. Berberine is an anti-inflammatory alkaloid used for the treatment of encephalomyelitis, lobar pneumonia, and lung abscess. Furthermore, matrine, oxymatrine, and harringtonines have been shown to exhibit antitumor activities in the treatment of tumors [19]. Principal component analysis (PCA) is a statistical method

that transforms a set of observed, possibly correlated variables into linearly independent variables (i.e., principal components) via orthogonal transformation. PCA can reveal the internal structure of data for better interpretation of data variables. As shown in Figure 3, FC and FTB samples were clearly separated along PC1 in both positive and negative ion modes but clustered tightly along PC1 within each group, which indicates that the metabolite profiles were significantly different between FTB and FC but similar within each group.

FTB

POS



NEG

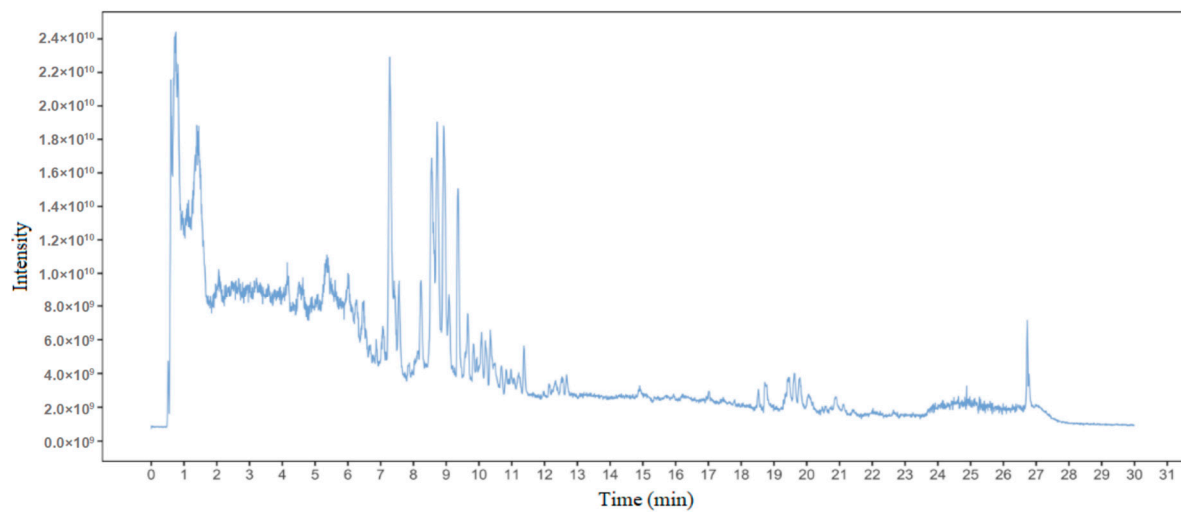
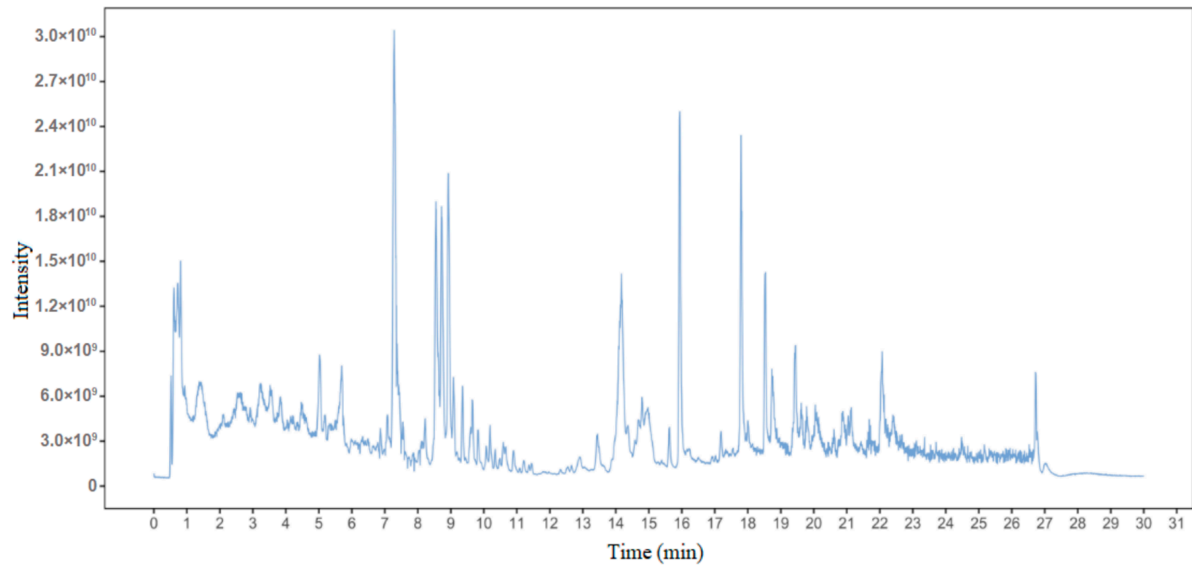


Figure 2. Cont.

FC

POS



NEG

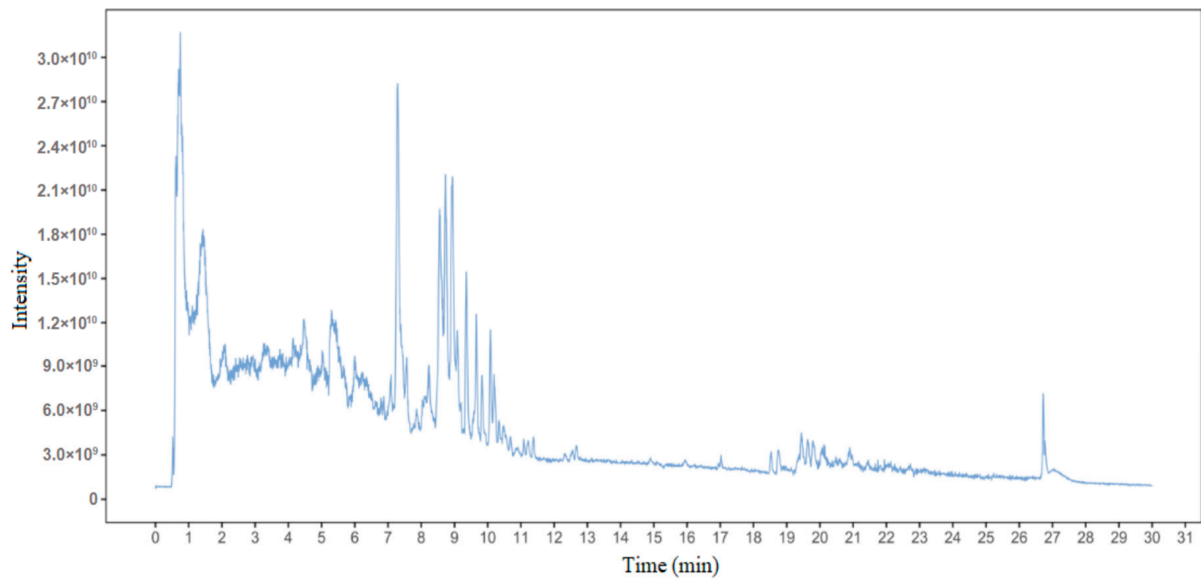


Figure 2. UHPLC-QE-MS TICs of FTB and FC in positive and negative ion modes.

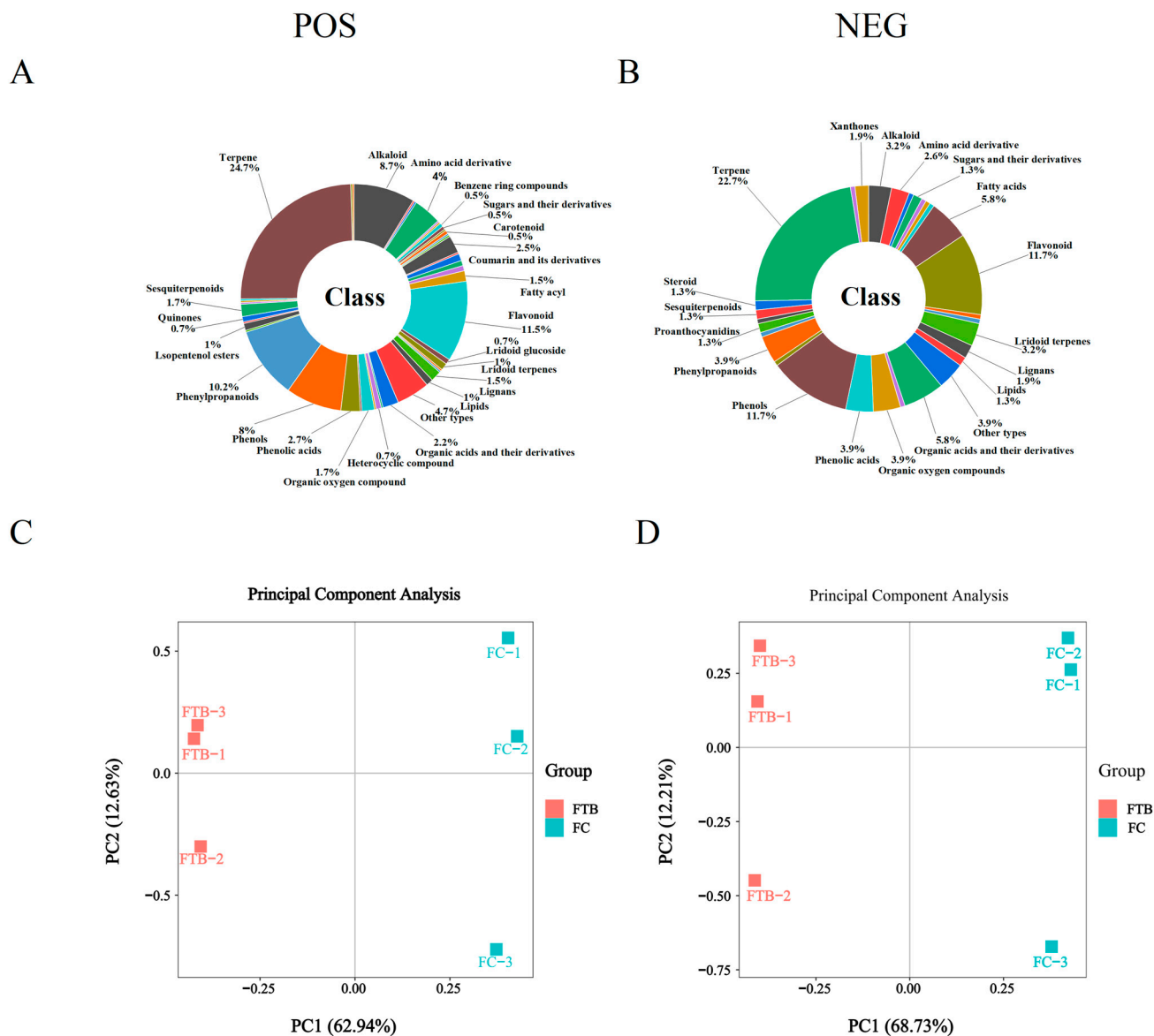


Figure 3. Schematic representation of the different classes (A,B) and PCA (The horizontal axis PC1 and the vertical axis PC2 represent the two directions where the data variation is greatest. Percentage represents the proportion of variation in each direction to the total variation.) of FTB and FC metabolites in the positive and negative ion modes (C,D).

3.3. Analysis of Differential Metabolites

Multivariate analysis focuses more on the relationships between metabolites and their agonistic/antagonistic effects in biological processes. By taking into account the results of both statistical analyses, we can examine the data from different perspectives and draw informed conclusions [20]. We identified distinct metabolites using Student's *t*-test with a significance threshold of $p < 0.05$ and a variable importance in projection (VIP) > 1 in the initial principal component of the OPLS-DA model. As shown in Figure 4, in the volcano plot, every point corresponds to a metabolite, with the *x*-axis showing the \log_2 fold change for each metabolite in the group and the *y*-axis representing the *p*-value of the *t*-test ($-\log_{10} n$). In the scatterplot, the size of the data points corresponds to the VIP value of the OPLS-DA model, with bigger points indicating higher VIP values. Data points are color-coded to indicate the final assessment of significance, with red representing significantly upregulated metabolites, blue representing significantly downregulated metabolites, and gray representing metabolites with no significant change. We found 110 differential metabolites

in the positive ion mode, of which 29 were upregulated and 81 were downregulated. These metabolites encompassed 23 classes of compounds, including flavonoids, phenols, iridoids, polyketides, lignans, phenylpropionoids, and amino acid derivatives. In the negative ion mode, a grand total of 87 distinct metabolites were detected, with 26 showing an increase in levels and 61 showing a decrease. These metabolites consisted of 15 classes of compounds, including flavonoids, terpenoids, phenols, phenylpropionoids, and amino acid derivatives.

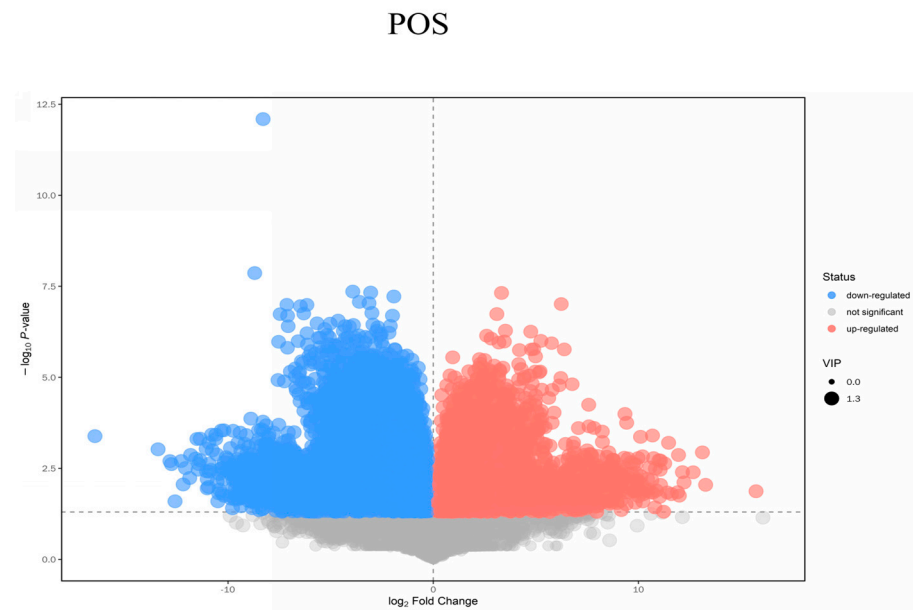
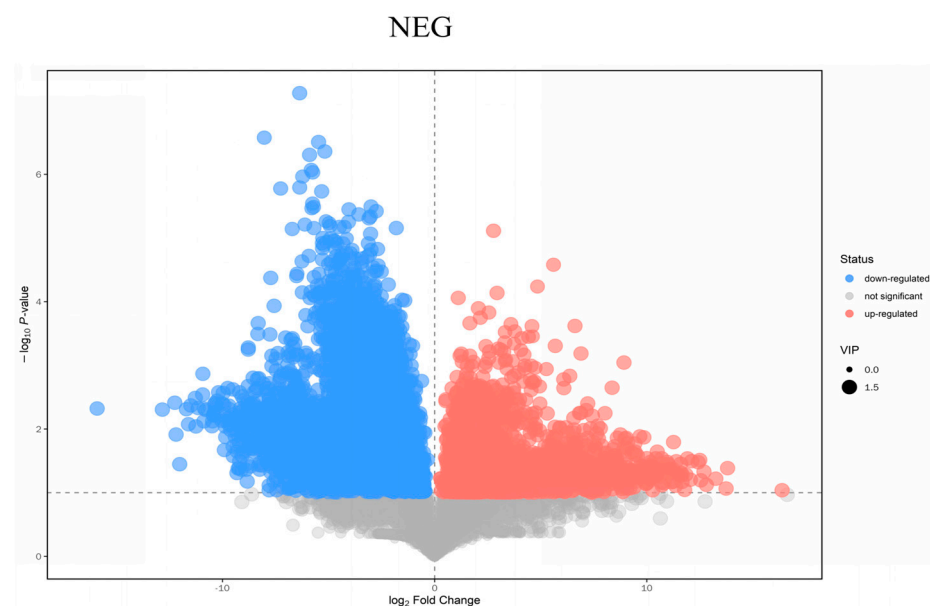
A**B**

Figure 4. Volcano plots of differential metabolites in positive (A) and negative ion modes (B).

Distinct metabolites frequently share comparable or supplementary biological roles and are controlled in a positive or negative manner by identical metabolic pathways, as in-

icated by exhibiting similar or contrasting expression profiles across various experimental sets. Hierarchical clustering allows the grouping of metabolites with similar characteristics and the identification of differences in metabolites among experimental groups. We performed complete-linkage clustering of differential metabolites by generating a Euclidean distance matrix (EDM) based on the quantitative expression of the differential metabolites and analyzed the top 20 differentially expressed metabolites (DEMs) (Figure 5) [21]. Each column and row of the heatmap correspond to each sample and metabolite, respectively. Color blocks show the metabolites' expression levels, with red representing high expression and blue representing low expression. Betulinic acid, L-asparagine, and polyphyllin VI were highly significant for differential expression markers in the positive ion mode. Betulinic acid is a pentacyclic triterpenoid abundant in plants of the genus *Betula*, such as birch bark. Pharmacological studies found that betulinic acid has anti-inflammatory, antitumor, anti-HIV, and anti-ulcer properties [22]. L-asparaginase specifically hydrolyzes the amide bond of asparagine and catalyzes the generation of aspartate and ammonia from asparagine. L-asparaginase can inhibit tumor growth by lowering the level of asparagine in vivo. Polyphyllin is the main active ingredient of Paris polyphylla and has been shown to mediate anti-inflammatory, antioxidant, antitumor, antibacterial, and antiemetic effects. Salidroside, ethyl gallate, and L-tryptophan were found to be highly significant in the negative ion mode for differentially expressed metabolites. Salidroside is a natural phytoalexin isolated from the rhizome of the Tibetan medicine *Rhodiola* with anti-inflammatory, antioxidant, antidepressant, antiradical, antitumor, and cardioprotective effects [23]. Reportedly, Ethyl gallate, found in the dried root extract of *Euphorbia fischeriana*, has shown potential in slowing the growth of cancer cells in liver, gastric, and breast cancers [24]. L-tryptophan is an optically active essential amino acid for the human body that exists in three isomers, namely L-tryptophan, D-tryptophan, and racemic tryptophan. It is used as a nutritional supplement for pregnant women and in special milk formula for infants. Furthermore, L-tryptophan can serve as a treatment for pellagra (chichism), as a sedative that regulates mental rhythm and improves sleep, and as one of the raw materials of Compound Amino Acid Injection [25].

We further plotted histograms of the relative abundance of several top DEMs and their chemical structures in Figure 6. Polyphyllin VI, betulinic acid, L-asparagine, gibberellic acid, and ethyl gallate were found to be the predominant compounds in FC, while (2R, 3R, 4S, 5S, 6R)-2-octoxy-6-[[[(2S, 3R, 4S, 5R)-3, 4, 5-trihydroxyoxan-2-yl]oxymethyl]oxane-3, 4, 5-triol was the most abundant in FTB according to our data.

Metabolic Pathway Analysis of Differential Metabolites

Organisms do not undergo complex metabolic reactions and their regulation in isolation; rather, they typically occur through intricate pathways and networks involving various genes and proteins. The interactions and mutual regulation between these genes and proteins ultimately lead to systematic changes in the metabolome. Hence, studying these metabolic and regulatory pathways can offer a more thorough and organized insight into the variations in biological processes caused by changes in experimental settings, along with the mechanisms behind traits or diseases and the effects of drugs. In biochemistry, a metabolic pathway refers to a series of biochemical reactions that occur during the enzymatic conversion of intracellular metabolites to new metabolites. A metabolic network is a system of metabolic reactions and control mechanisms that explain the metabolic and physiological activities within cells. Analysis of KEGG data showed that the differentially expressed metabolites were highly represented in 22 metabolic pathways, with 5 pathways in the positive ion mode and 18 in the negative ion mode [26]. According to the pathway network diagrams, positive ion mode DEMs were found to be abundant in metabolic pathways, secondary metabolite biosynthesis, and amino acid biosynthesis (Figure 7A). Conversely, negative mode DEMs showed significant associations with metabolic pathways, secondary metabolite biosynthesis, and carbon metabolism (Figure 7B).

A

POS

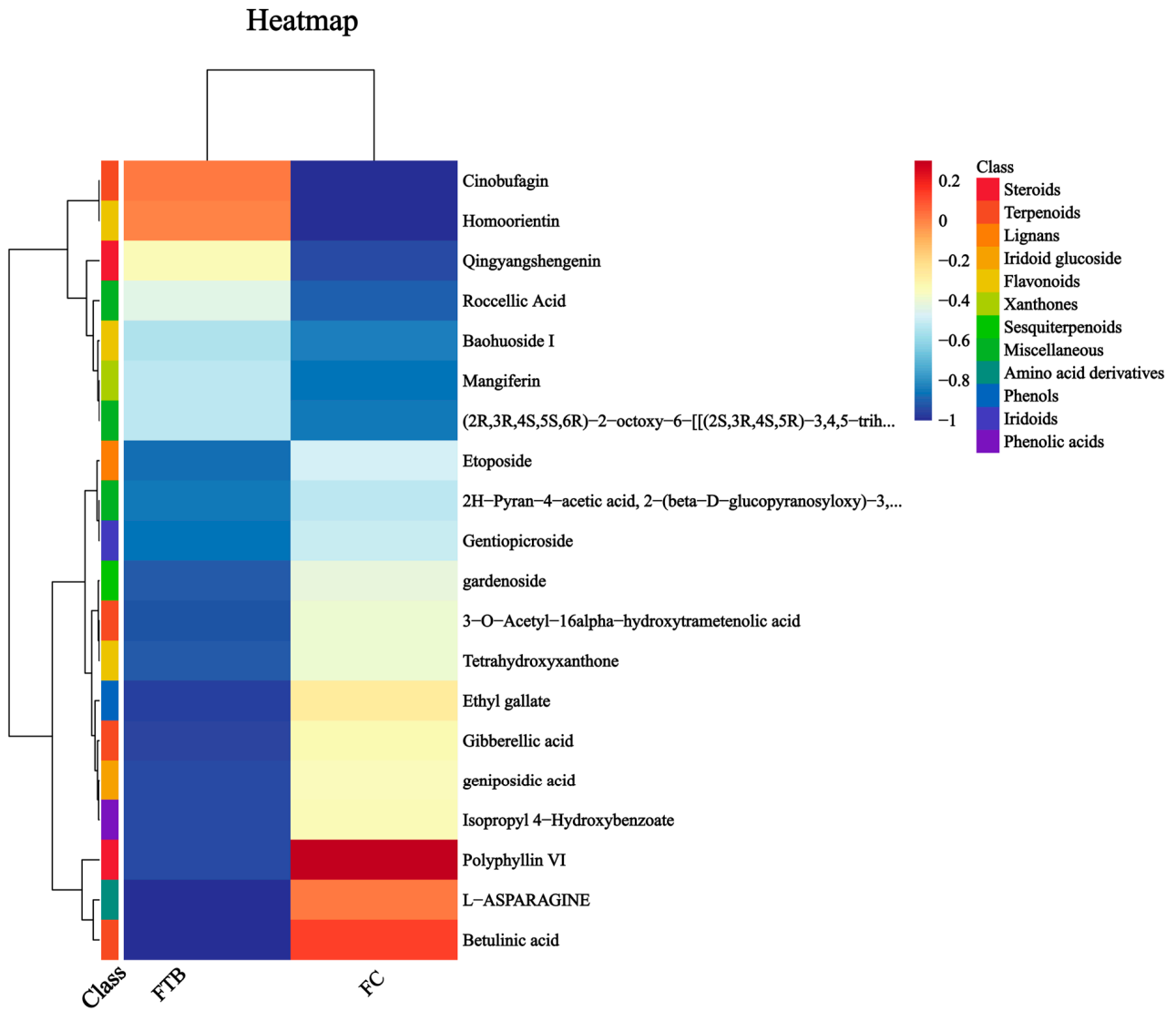


Figure 5. Cont.

B

NEG

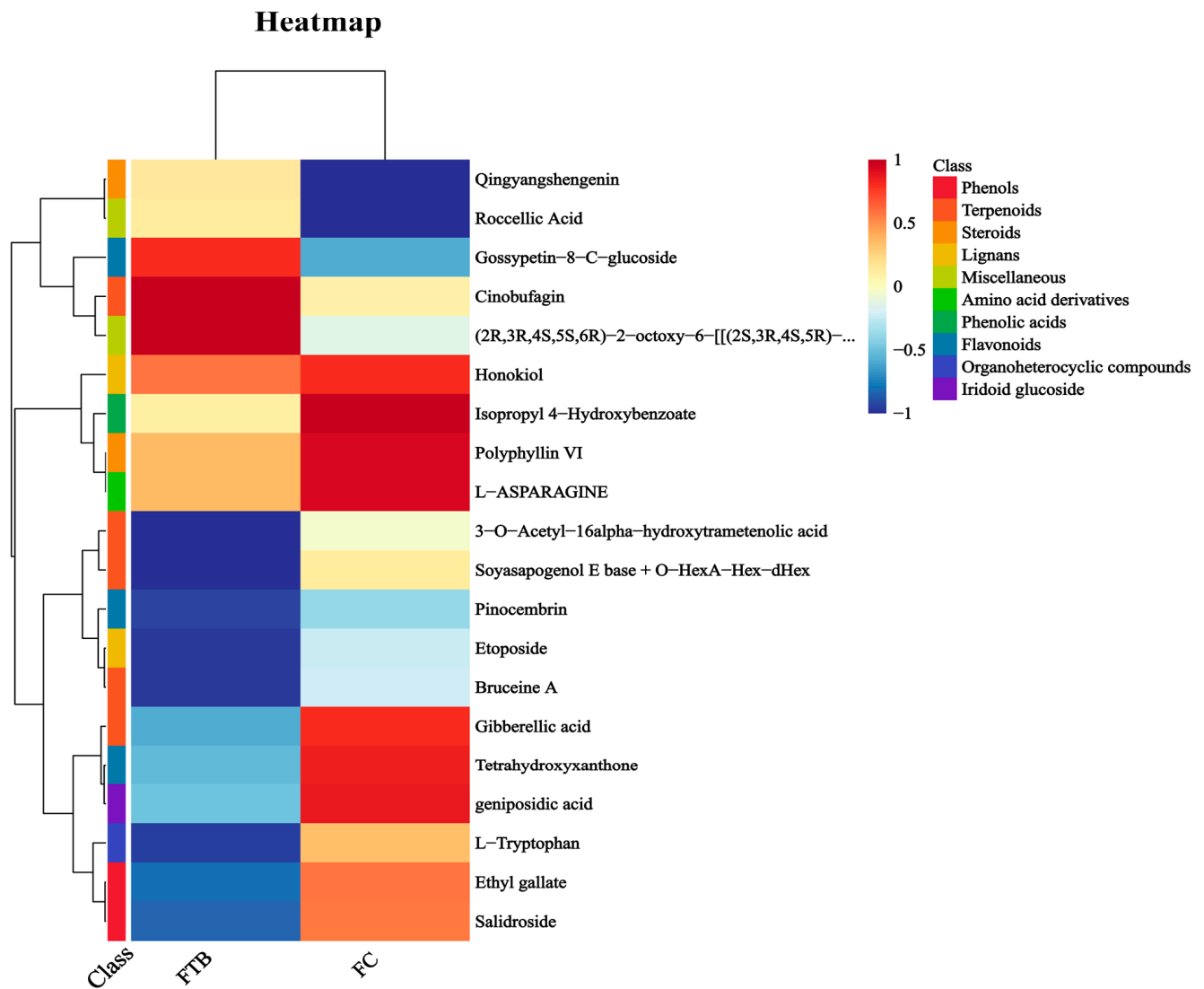


Figure 5. Heatmaps of the top 20 DEMs in positive and negative ions (each sample is represented by a column, each metabolite is visualized in a row, color blocks at different locations represent the relative expression of metabolites at the corresponding position, red indicates high expression of this substance content, and blue indicates low expression content; The seventh compound in (A) and the fifth compound in (B) are all called: (2R, 3R, 4S, 5S, 6R)-2-Octoxy-6-[[[(2S, 3R, 4S, 5R)-3,4,5-trihydroxyoxan-2-yl]oxymethyl]oxane-3,4,5-triol]; The full name of the ninth compound in (A): 2H-Pyran-4-acetic acid, 2-(beta-D-glucopyranosyloxy)-3,4-dihydro-3-(2-hydroxyethylidene)-5-(methoxycarbonyl)-, 2-(4-hydroxyphenyl) ethyl ester, (2S, 3Z, 4S)).

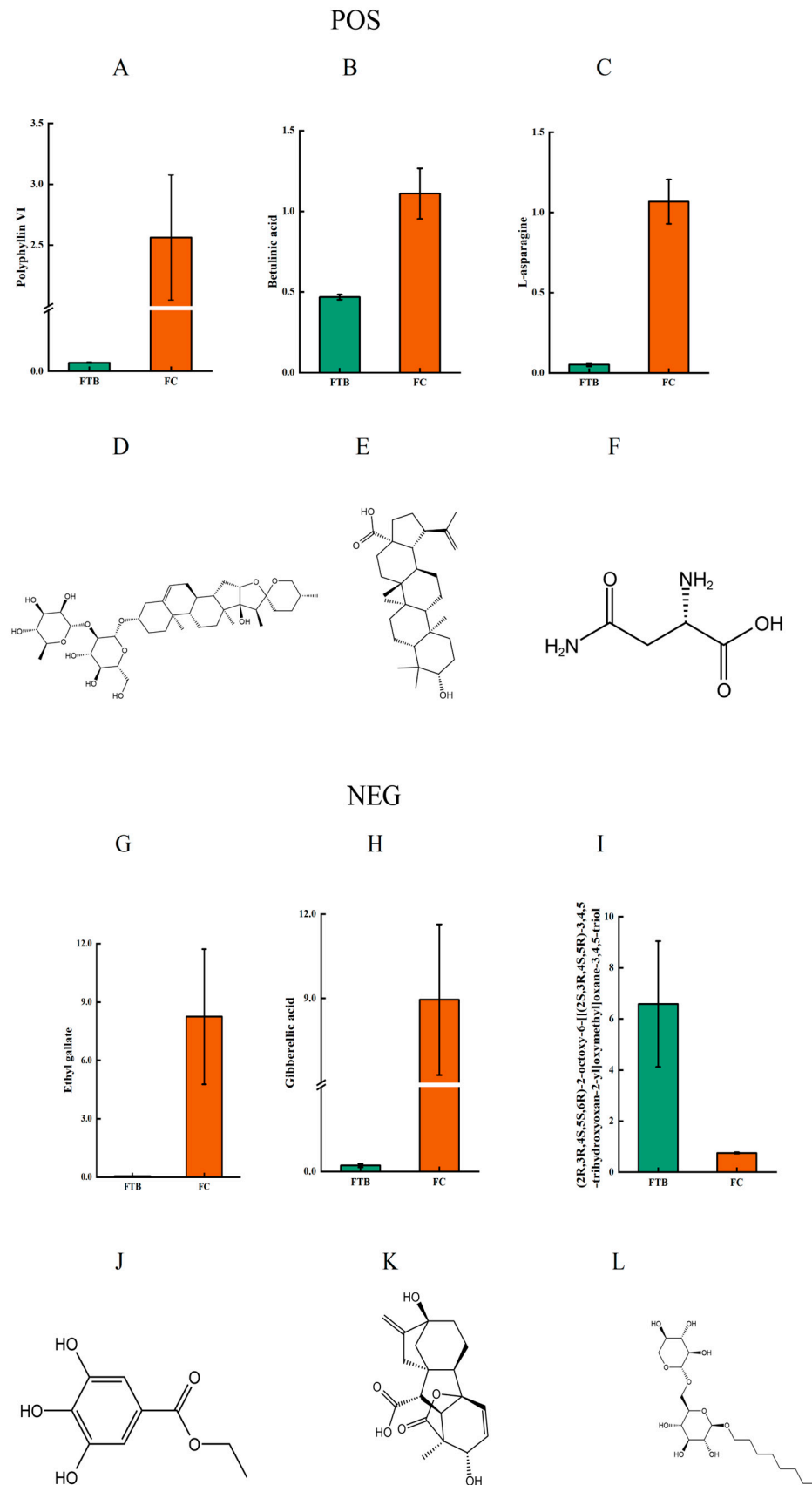


Figure 6. Histograms of top DEMs in positive (A–C) and negative (G–I) ion modes; structural formulae of top DEMs (D–F,J–L).

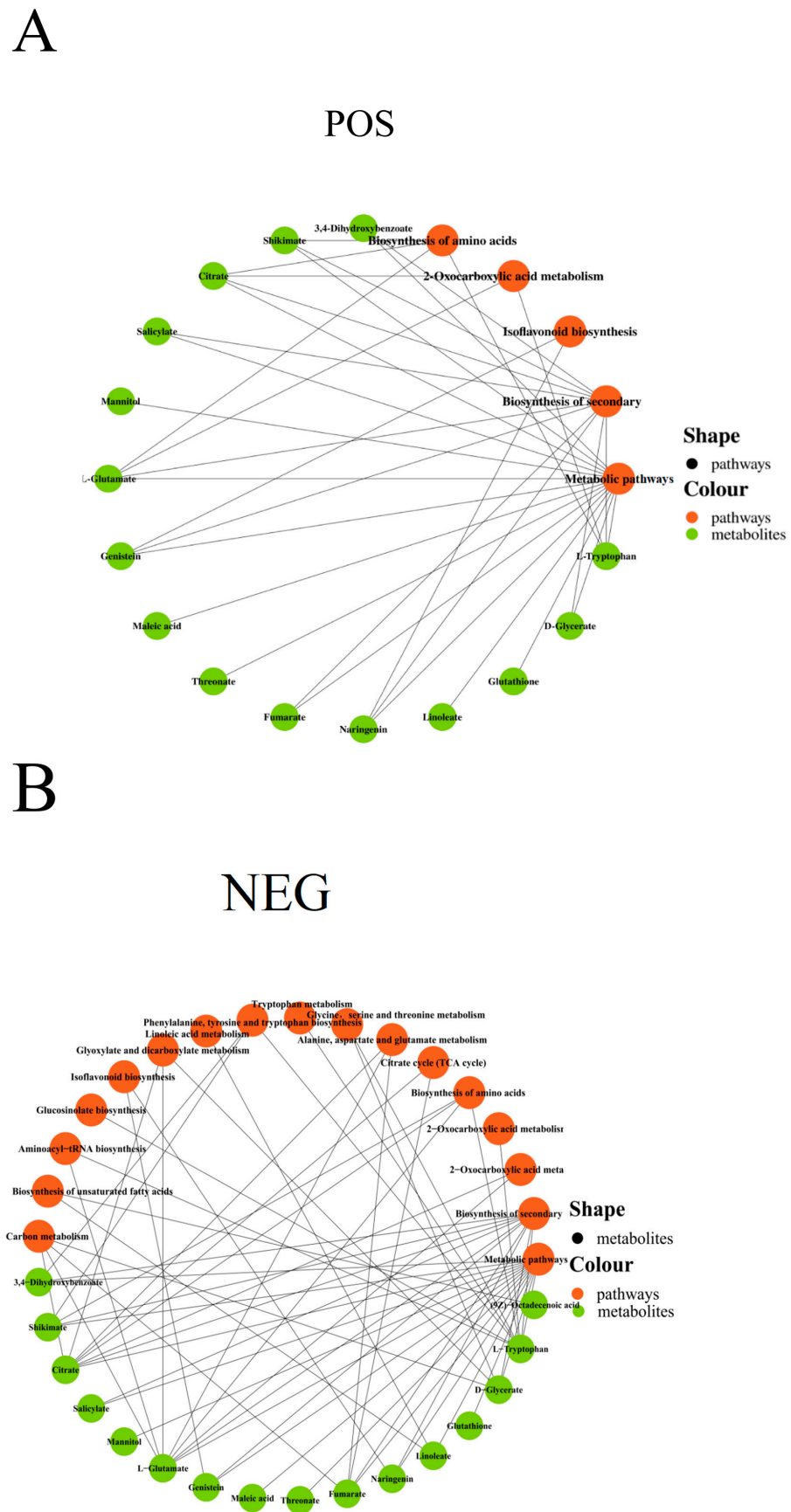


Figure 7. KEGG network diagrams of DEMs in positive (A) and negative ion modes (B). Orange nodes represent pathways and green nodes represent metabolites.

4. Discussion

The study conducted a comparative analysis of the metabolic profiles of FC and FTB, revealing that flavonoids, phenolic acids, and alkaloids were the most abundant differentially expressed metabolites. Flavonoids, which are commonly present in plants and are abundant in various TCM herbs, are a group of natural organic compounds characterized by a fundamental C₁₅ benzene ring structure of C₆-C₃-C₆. For example, liquiritigenin (flavonoid) in FC and FTB have antioxidant and anti-inflammatory activities and can prevent arsenic trioxide (ATO)-induced hepatotoxicity [27]. Phenolic acids are a class of natural active products in plants with anti-inflammatory, antioxidant, antitumor, and antibacterial properties. Their biosynthesis mainly involves the shikimic acid and phenyl-propionic acid metabolic pathways. Studies have shown that both FC and FTB have high levels of protocatechuic acid, gallic acid, and shikimic acid. Protocatechuic acid, a type of phenolic acid found in fruits and vegetables, has the ability to efficiently eliminate and decrease the amounts of reactive oxygen species (ROS) within cells, leading to a decrease in cell damage and apoptosis. Furthermore, protocatechuic acid has the ability to reduce inflammation by decreasing the production of cancer-causing substances like tumor necrosis factor- α (TNF- α) and interleukin-1 β , as well as easing inflammation. Gallic acid exists as a free lipid or lipid compound in FC and has been reported to exhibit antioxidant, anticancer, hypoglycemic, hypolipidemic, antibacterial, antiviral, and anti-inflammatory activities [28]. The gallic acid in FC fruit extract can reduce the number of immortalized and cancerous cells by inhibiting the rate of cell proliferation [29]. Additionally, gallic acid exhibits strong inhibitory properties against α -amylase and α -glucosidase, making it a potential hypoglycemic treatment. Oxalic acid is an organic compound that can inhibit platelet aggregation and arterial, venous, and cerebral thrombosis by modulating the metabolism of arachidonic acid. Due to its anti-inflammatory and analgesic properties, oxalic acid has been utilized as a precursor in the development of antiviral and anticancer medications [30]. FC and FTB are rich in alkaloids such as nuciferine, betaine, and cephalotaxine. Nuciferine is an aporphine alkaloid with diverse pharmacological and therapeutic effects. It not only lowers blood lipid levels, scavenges free radicals, and prevents hypercholesterolemia and atherosclerosis, but also exhibits antimitotic and potent antibacterial activities [31]. Betaine, also known as N, N, N-trimethylglycine, is an alkaloid that has been shown to inhibit tumor growth, lower blood pressure, prevent peptic ulcer and gastrointestinal dysfunction, and ameliorate liver diseases [32]. Cephalotaxine is an alkaloid extracted from *Cephalotaxus fortunei* or other plants of the Cephalotaxaceae family. The alkaloid has the ability to block protein production in eukaryotic cells, break down polyribosomes, and act as an anticancer drug by disrupting protein synthesis. Clinically, it is utilized for treating acute promyelocytic leukemia, acute monocytic leukemia, acute granulocytic leukemia, and malignant lymphomas [33]. By performing KEGG pathway analysis on the compounds, we identified 22 signaling pathways, and most of the differentially expressed metabolites are present in metabolic pathways and in the biosynthesis of secondary metabolites, which may account for the differences in metabolites between FC and FTB. Citrate, Shikimate, Mannitol, L-Glutamate, Maleic acid, Threonate, etc., are mainly related to the metabolic pathway of secondary metabolites. L-Tryptophan, D-Glycerate, Glutathione, Mannitol, Salicylate, and Linoleate are mainly related to metabolic pathways. Metabolic pathways are chemical cascades that occur within cells and can be categorized into anabolic pathways (energy-consuming synthesis of complex molecules) or catabolic pathways (energy-releasing breakdown of complex molecules). These two pathways are complementary since the energy released by one pathway can be consumed by the other. The degradation processes in the catabolic pathways provide the energy required for biosynthesis in the anabolic pathways. Hence, phytochemicals like flavonoids, terpenes, phenolic compounds, and carotenoids play a crucial role in promoting human well-being by offering antioxidant, anticancer, anti-AIDS, antibacterial, anti-allergy, and anti-inflammatory benefits [34].

5. Conclusions

Some studies have suggested that phenolic acids, terpenoids, and flavonoids are the primary active ingredients that mediate the pharmacological activities of FC. The components found in medicinal plants serve as the foundation for the healing properties of traditional Chinese medicine, with their build-up being closely tied to specific locations and periods of time. The present study may serve as a basis for subsequent research on the biosynthetic pathways and related biological activities of FC and provide guidance for the clinical application of TCM. Although our study has identified DEMs between FC and FTB, further research and development are warranted for elucidating the chemical composition, biological activity, and clinical application of FC, especially the pharmacological activities of the different components of FC.

Supplementary Materials: The following supporting information can be downloaded at: <https://www.mdpi.com/article/10.3390/app14073123/s1>, Table S1: Seed data; Table S2: POS_final; Table S3: NEG_final.

Author Contributions: Conceptualization: H.G.; Methodology: H.G.; Data curation: H.G.; Formal analysis: Y.S.; Investigation: Y.S. and H.G.; Software: Y.S.; Validation: Y.S.; Supervision: Y.S.; Funding acquisition: H.G.; Writing—original draft: Y.S.; Writing—review & editing: Y.S. and H.G.; Project administration: H.G.; Resources: H.G. All authors have read and agreed to the published version of the manuscript.

Funding: This research received no external funding.

Data Availability Statement: The data is included in the article or in the supplementary information.

Acknowledgments: Our gratitude goes to Kevin Nyberg from Northwestern University for his help in editing the manuscript for English language and grammar.

Conflicts of Interest: The authors declare no conflict of interest.

References

1. Zhang, Y.; Liu, X.; Gao, S.; Qian, K.; Liu, Q.; Yin, X. Research on the neuro-protective compounds in *Terminalia chebula* retz extracts in-vivo by UPLC-QTOF-MS. *Acta Chromatogr.* **2017**, *30*, 169–174. [[CrossRef](#)]
2. Singamaneni, V.; Dokuparthi, S.K.; Banerjee, N.; Kumar, A.; Chakrabarti, T. Phytochemical Investigation and Antimutagenic Potential of Ethanolic Extracts of *Emblia officinalis*, *Terminalia chebula* and *Terminalia bellirica*. *Nat. Prod. J.* **2020**, *10*, 488–494. [[CrossRef](#)]
3. Muneer, A.; Alhowail, A.; Aldubayan, M.; Rabbani, S.I. The activity of *Terminalia chebula* Retz. extract on doxorubicin-induced renal damage in rats. *J. Pharm. Pharmacogn. Res.* **2020**, *8*, 237–246. [[CrossRef](#)] [[PubMed](#)]
4. Sheng, Z.; Zhao, J.; Muhammad, I.; Zhang, Y. Optimization of total phenolic content from *Terminalia chebula* Retz. fruits using response surface methodology and evaluation of their antioxidant activities. *PLoS ONE* **2018**, *13*, e0202368. [[CrossRef](#)] [[PubMed](#)]
5. Ekambaram, S.P.; Babu, K.B.; Perumal, S.S.; Rajendran, D. Repeated oral dose toxicity study on hydrolysable tannin rich fraction isolated from fruit pericarps of *Terminalia chebula* Retz in Wistar albino rats. *Regul. Toxicol. Pharmacol.* **2018**, 92182–92188. [[CrossRef](#)] [[PubMed](#)]
6. Yang, Y.; Gesang, S.; Wu, J. Review of plant classification and pharmaceutical characteristics of Quixote, Quixote and Gansu. *Appl. Med. Biotechnol. China* **2004**, *01*, 14–28.
7. Li, D.; Zhu, W.; Duan, S.; Lai, Y. Determination of half-lethal amount of bark alcohol extract and its effect on intestinal muscle. *J. Dali Univ.* **2014**, *13*, 10–13.
8. Zhou, K.; Jian, P.; Liang, W.; Liang, L.; Ye, T.; Chang, Z.; Zhang, Q.; Zhang, L. Analysis of the chemical composition of the Tibetan herbs and the Tibetan Quixote based on UPLC-Q-Exact Orbitrap-MS. *J. Chin. Mass Spectrom.* **2020**, *41*, 254–267.
9. Lee, H.S.; Jung, S.H.; Yun, B.S.; Lee, K.W. Isolation of chebulic acid from *Terminalia chebula* Retz and its antioxidant effect in isolated rat hepatocytes. *Arch Toxicol* **2007**, *81*, 211–218. [[CrossRef](#)]
10. Lin, M.C.; Yin, M.C. Preventive effects of ellagic acid against doxorubicin-induced cardio-toxicity in mice. *Cardiovasc. Toxicol.* **2013**, *13*, 185–193. [[CrossRef](#)]
11. Lee, J.; Nho, Y.H.; Yun, S.K.; Hwang, Y.S. Use of ethanol extracts of *Terminalia chebula* to prevent periodontal disease induced by dental plaque bacterial. *BMC Complement. Altern. Med.* **2017**, *17*, 113–119. [[CrossRef](#)] [[PubMed](#)]
12. Nayak, S.S.; Ankola, A.V.; Metgud, S.C.; Bolmal, U.K. An in vitro study to determine the effect of *Terminalia chebula* extract and its formulation on *Streptococcus mutans*. *J. Contemp. Dent. Pract.* **2014**, *15*, 278–282. [[CrossRef](#)] [[PubMed](#)]

13. Shankara, B.R.; Ramachandra, Y.L.; Rajan, S.S.; Ganapathy, P.S.; Yarla, N.S.; Richard, S.A.; Dhananjaya, B.L. Evaluating the anticancer potential of ethanolic gall extract of *Terminalia chebula* (Gaertn.) Retz. (combretaceae). *Pharmacogn. Res.* **2016**, *8*, 209–212. [[CrossRef](#)] [[PubMed](#)]
14. Messeha, S.S.; Zarmouh, N.O.; Taka, E.; Gendy, S.G.; Shokry, G.R.; Kolta, M.G.; Soliman, K.F.A. The role of monocarboxylate transporters and their chaperone CD147 in lactate efflux inhibition and the anticancer effects of *Terminalia chebula* in neuroblastoma cell line N2-A. *Eur. J. Med. Plants* **2016**, *12*, EJM.P.23992. [[CrossRef](#)] [[PubMed](#)]
15. Saha, A.K.; Das, S.K.; Kar, N.B. Antijuvenoid Action of Terpenoid Imidazole Compound on Larval–Pupal–Adult Development of Silkworm, *Bombyx mori* L. *Int. J. Ind. Entomol.* **2007**, *14*, 127–135.
16. Al-Maharik, N.; Jaradat, N.; Bassalat, N.; Hawash, M.; Zaid, H. Isolation, Identification and Pharmacological Effects of *Mandragora autumnalis* Fruit Flavonoids Fraction. *Molecules* **2022**, *27*, 1046. [[CrossRef](#)] [[PubMed](#)]
17. Razola-Díaz, M.D.C.; Aznar-Ramos, M.J.; Benítez, G.; Gómez-Caravaca, A.M.; Verardo, V. Exploring the potential of phenolic and antioxidant compounds in new Rosaceae fruits. *J. Sci. Food Agric.* **2024**, *104*, 3705–3718. [[CrossRef](#)] [[PubMed](#)]
18. Niu, F.; Du, Y.; Huang, Y.; Zhou, H.; Liu, J. Progress in the synthesis of phenylpropanoid acid compounds and its derivatives by engineered microorganisms. *Synth. Biol.* **2020**, *1*, 337–357.
19. Meng, Q.; Liang, J.; Wu, G.; Lu, H. Progress in the pharmacological effects of alkaloid compounds. *Shizhen Natl. Med.* **2003**, *11*, 700–702.
20. Saccenti, E.; Hoefsloot, H.C.; Smilde, A.K.; Westerhuis, J.A.; Hendriks, M.M. Reflections on univariate and multivariate analysis of metabolomics data. *Metabolomics* **2014**, *10*, 361–374. [[CrossRef](#)]
21. Kolde, R. *Pheatmap: Pretty Heatmaps*, R Package version 061; The Comprehensive R Archive Network (CRAN): Vienna, Austria, 2015.
22. Zhao, X.; Li, Y.; Zhang, J. Effect of betulinic acid 51 on oxidative damage and apoptosis of PC12H₂O. *J. Med. Mol. Biol.* **2021**, *18*, 428–433.
23. Li, Y.R.; Cao, W.; Guo, J.; Miao, S.; Ding, G.R.; Li, K.C.; Wang, J.; Guo, G.Z. Comparative investigations on the protective effects of rhodioid, ciwujianoside-B and astragaloside IV on radiation injuries of the hematopoietic system in mice. *Phytother. Res.* **2011**, *25*, 644–653. [[CrossRef](#)] [[PubMed](#)]
24. Cui, H.; Wang, M.; Yuan, J.; Liu, J. Effect of ethyl gallate on invasion abilities and its mechanism of breast cancer MDA-MB-231 cells. *Yao Xue Xue Bao = Acta Pharm. Sin.* **2015**, *50*, 45–49.
25. Liu, Q.; Shi, Z.; Wu, J.; Huang, B.; Liang, X.; Cui, X.; Hu, S.; Niu, S.; Kong, W. Analysis of associated substances and major metabolic pathways for the development of pellagra lateral ear fruiting bodies based on non-target metabolomics. *J. Bact.* **2024**, *43*, 59–73. [[CrossRef](#)]
26. Dai, M.; Jiang, Z.; Huang, X. Progress in the physiological function of tryptophan and metabolites and its role in disease. *Zhongnan Pharm.* **2021**, *19*, 909–915.
27. Keranmu, A.; Pan, L.B.; Fu, J.; Han, P.; Yu, H.; Zhang, Z.W.; Xu, H.; Yang, X.-Y.; Hu, J.-C.; Zhang, H.-J.; et al. Biotransformation of Liquiritigenin into Characteristic Metabolites by the Gut Microbiota. *Molecules* **2022**, *27*, 3057. [[CrossRef](#)] [[PubMed](#)]
28. Reddy, D.N.; Huang, F.Y.; Wang, S.P.; Kumar, R. Synergistic Antioxidant and Antibacterial Activity of Curcumin-c3 Encapsulated Chitosan Nanoparticles. *Curr. Pharm. Des.* **2020**, *26*, 5021–5029. [[CrossRef](#)] [[PubMed](#)]
29. Luan, X.; Ou, W.; Hu, J.; Lu, J. Gallic acid alleviates lipopolysaccharide-induced renal injury in rats by inhibiting cell pro-death and inflammatory response and its mechanism. *Cell. Mol. Biol.* **2023**, *69*, 31–35. [[CrossRef](#)]
30. Aleixandre, A.; Gil, J.V.; Sineiro, J.; Rosell, C.M. Understanding phenolic acids inhibition of α -amylase and c-glucosidase and influence of reaction conditions. *Food Chem.* **2022**, *372*, 1231. [[CrossRef](#)]
31. Xu, H.; Lyu, X.; Guo, X.; Yang, H.; Duan, L.; Zhu, H.; Pan, H.; Gong, F.; Wang, L. Distinct AMPK-Mediated FAS/HSL Pathway Is Implicated in the Alleviating Effect of Nuciferine on Obesity and Hepatic Steatosis in HFD-Fed Mice. *Nutrients* **2022**, *14*, 1898. [[CrossRef](#)]
32. Bolik, S.; Schlaich, A.; Mukhina, T.; Amato, A.; Bastien, O.; Schneck, E.; Demé, B.; Jouhet, J. Lipid bilayer properties potentially contributed to the evolutionary disappearance of betaine lipids in seed plants. *BMC Biol.* **2023**, *21*, 275. [[CrossRef](#)] [[PubMed](#)]
33. Whaun, M.J.; Brown, D.N. Treatment of chloroquine-resistant malaria with esters of cephalotaxine: Homoharringtonine. *Ann. Trop. Med. Parasitol.* **2016**, *84*, 229–237. [[CrossRef](#)]
34. Cui, W.; Bai, X.; Wang, J.; Jin, H. Progress in the regulation of abscisic acid and the biosynthesis of secondary metabolites related to plant disease resistance. *Bot. Med.* **2022**, *1*, 1–11. [[CrossRef](#)]

Disclaimer/Publisher’s Note: The statements, opinions and data contained in all publications are solely those of the individual author(s) and contributor(s) and not of MDPI and/or the editor(s). MDPI and/or the editor(s) disclaim responsibility for any injury to people or property resulting from any ideas, methods, instructions or products referred to in the content.